

# The Effect of a High Temperature Superconducting Patch on a Rectangular Microstrip Antenna

Fouad Chebbara\*, Mounir Amir\* and Tarek Fortaki\*

**Abstract** – The complex resonant frequency problem of a superconductor patch is formulated in terms of an integral equation which is the kernel of a dyadic Green's function. To include the effect of the superconductivity of the microstrip patch, the surface complex impedance of the superconductor film is introduced using the two fluids model of Gorter and Casimir. The Galerkin procedure is used in the resolution of the electric field integral equation. Numerical results concerning the effect of the operating temperature of a superconductor patch on the characteristics of the antenna are presented.

**Keywords:** HTS microstrip patch, Microstrip antenna, Superconducting patch, Dyadic Green's function, Galerkin procedure

## 1. Introduction

In recent years, a great deal of interest has been observed in the development and use of high temperature superconducting materials (HTS) in microwave technology, such as resonators, filters and antennas. This is due to their low resistance and relatively high reactance. They show superior performance and characteristics to a normal conductor's devices, such as lower power losses, reduced attenuation and noise level and, moreover, the propagation time of signals in the circuit can be greatly reduced [1]-[2]-[3]-[4]-[5].

The resonant characteristics of High  $T_c$  superconducting microstrip antennas was first studied by Richard *et al.* [4] using the cavity model. Since the cavity model does not consider rigorously the effects of surface waves and fringing fields at the edge of the patch [6], in this work, the physical parameters of the antenna are replaced with effective ones in order to line up the obtained theoretical results with the measured data. Recently, Silva *et al.* [5] has studied the resonant characteristics of High  $T_c$  superconducting microstrip antennas using full-wave analysis. It is noted that in this work, the bandwidth for an HTS microstrip patch antenna as function of the operating temperature is incorrect.

This paper investigates the effect of thin superconducting patch loading on the resonant frequency and bandwidth of a rectangular microstrip structure as illustrated in Fig. 1. The complex resonant frequency problem considered here is formulated in terms of an integral equation using vector Fourier transforms [7]. The surface impedance of the superconductor film is modeled using Gorter and Casimir's two fluid model [3]-[5]-[8]. This paper is organized as follows. First, the integral equation for the

unknown patch currents is formulated. The derivation is performed in the Fourier transform domain and utilized the dyadic Green's function of the considered structure, without taking into account the effect of superconductivity. To include the superconductivity effect of the patch, a surface complex impedance,  $Z_s$  is considered. The Galerkin moment method is used to solve the integral equation. The characteristic equation for complex resonant frequencies is given. Various numerical results are given in section 3. Finally, conclusions are summarized in section 4.

## 2. Analysis Method

Fig. 1 illustrates the problem to be solved. We have a rectangular superconducting patch with dimensions  $(a, b)$  and a thickness  $R$ , is printed on a dielectric substrate isotropic of thickness  $d$ , is characterized by a free space permeability  $\mu_0$  and a permittivity  $\epsilon$ . The ambient medium is air with constitutive parameters  $\mu_0$  and  $\epsilon_0$ . Assuming an  $e^{j\omega t}$  time variations and starting from Maxwell's equations in the Fourier transform domain, we can show that the transverse fields inside the  $j$  layer ( $Z_{j-1} < Z < Z_j$ ) can be written in terms of the longitudinal components  $\tilde{E}_z$  and  $\tilde{H}_z$  as [9]-[10].

$$\tilde{E}(k_s, z) = \begin{bmatrix} \tilde{E}_x(k_s, z) \\ \tilde{E}_y(k_s, z) \end{bmatrix} = \bar{F}(k_s) \cdot \begin{bmatrix} \frac{1}{k_s} \frac{\partial \tilde{E}_z(k_s, z)}{\partial z} \\ \frac{\omega \mu_0}{k_s} \tilde{H}_z(k_s, z) \end{bmatrix}$$

$$\tilde{E}(k_s, z) = \bar{F}(k_s) \cdot \mathcal{E}(k_s, z) \quad (1)$$

\* Dept. of Electronics University of Batna, 05000, Banta, Algeria  
(fouadchebbara@hotmail.com)

Received 4 November, 2008 ; Accepted 22 April, 2009

$$\tilde{H}(k_s, z) = \begin{bmatrix} \tilde{H}_y(k_s, z) \\ -\tilde{H}_x(k_s, z) \end{bmatrix} = \bar{F}(k_s) \cdot \begin{bmatrix} \frac{\omega \epsilon_j}{k_s} \tilde{H}_z(k_s, z) \\ \frac{1}{k_s} \frac{\partial \tilde{H}_z(k_s, z)}{\partial z} \end{bmatrix}$$

$$\tilde{H}(k_s, z) = \bar{F}(k_s) \cdot h(k_s, z) \quad (2)$$

**e** and **h** are, respectively, the transverse electric and magnetic fields in the (TM, TE) representation, and

$$\bar{F}(k_s) = \frac{1}{k_s} \begin{bmatrix} k_x & k_y \\ k_y & -k_x \end{bmatrix} \quad (3)$$

with:

$$k_s^2 = k_x^2 + k_y^2$$

Substituting the expressions of  $\tilde{E}_z$  and  $\tilde{H}_z$  [8]-[9] into (1) and (2), we get

$$\tilde{E}_z = A e^{-ik_z Z} + B e^{ik_z Z} \quad (4)$$

$$\tilde{H}_z = \bar{g}(k_s) \cdot [A e^{-ik_z Z} - B e^{ik_z Z}] \quad (5)$$

In (4) and (5), **A** and **B** are two-component unknown vectors and

$$\bar{g}(k_s) = \text{diag} \left[ \frac{\omega \epsilon}{k_z}, \frac{k_z}{\omega \mu} \right] \quad (6)$$

Writing (4) and (5) in the planes  $z = z_{j-1}$  and  $z = z_j$ , and by eliminating the unknowns A and B, we obtain the matrix form

$$\begin{bmatrix} e(k_s, z_j^-) \\ h(k_s, z_j^-) \end{bmatrix} = \bar{T}_j \cdot \begin{bmatrix} e(k_s, z_{j-1}^+) \\ h(k_s, z_{j-1}^+) \end{bmatrix} \quad (7)$$

With:

$$\bar{T}_j = \begin{bmatrix} \bar{T}_j^{11} & \bar{T}_j^{12} \\ \bar{T}_j^{21} & \bar{T}_j^{22} \end{bmatrix}$$

$$\bar{T}_j = \begin{bmatrix} \cos(k_{zj} d_j) & -i \bar{g}^{-1} \cdot \sin(k_{zj} d_j) \\ -i \bar{g} \cdot \sin(k_{zj} d_j) & \cos(k_{zj} d_j) \end{bmatrix} \quad (8)$$

Which combines **e** and **h** on both sides of the  $j^{\text{th}}$  layer as input and output quantities. The matrix  $\bar{T}_j$  is the matrix representation of the  $j^{\text{th}}$  layer in the (TM, TE) representation.

The boundary conditions for the considered structure presented in Fig.1 in the spectral domain

$$\bar{e}_1(k_s, z_0^+) = \bar{0} \quad (9)$$

$$\begin{bmatrix} \bar{e}_2(k_s, z_1^+) \\ \bar{h}_2(k_s, z_1^+) \end{bmatrix} = \bar{T}_1 \cdot \begin{bmatrix} \bar{e}_1(k_s, z_0^+) \\ \bar{h}_1(k_s, z_0^+) \end{bmatrix} - \begin{bmatrix} 0 \\ \bar{J}(z_1) \end{bmatrix} \quad (10)$$

$$\bar{h}_2(k_s, z_1^+) = \bar{g}_0(k_s) \bar{e}_2(k_s, z_1^+) \quad (11)$$

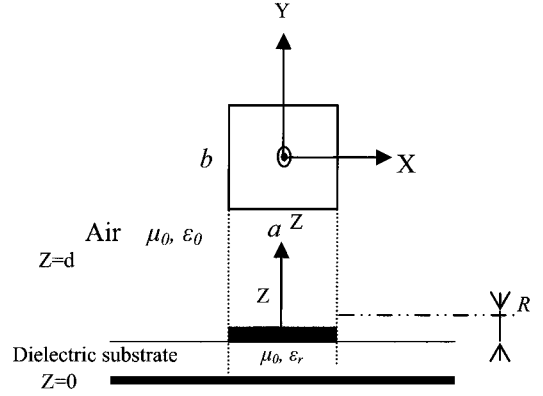


**Fig. 1.** Geometrical structure of a superconducting rectangular microstrip patch

The transformed components of the tangential electric field are expressed as a function of the transformed current density components on the patch, as

$$\begin{bmatrix} \tilde{E}_x \\ \tilde{E}_y \end{bmatrix} = \begin{bmatrix} G_{xx} & G_{xy} \\ G_{yx} & G_{yy} \end{bmatrix} \cdot \begin{bmatrix} \tilde{J}_x \\ \tilde{J}_y \end{bmatrix} \quad (12)$$

To include the effect of the superconducting of the microstrip film, the dyadic Green's function is modified by considering a surface complex impedance  $Z_s$ , and is determinate by using the model of Gorter and Casimir [3]-[5]-[8].

$$Z_s = \sqrt{\frac{\omega \mu_0}{2\sigma}} \quad (13)$$

If the thickness of the superconducting film  $R$  is less than three penetration depths, a better boundary condition is given by [3]

$$Z_s = \frac{1}{R \cdot \sigma} \quad (14)$$

Where the complex conductivity is given by [3]-[5]

$$\sigma = \sigma_n \left( \frac{T}{T_C} \right)^4 + \left( \left( 1 - \left( \frac{T}{T_C} \right)^4 \right) / \left( i \omega \mu_0 \lambda_0^2 \right) \right) \quad (15)$$

The electric field and the surface current densities total in the interface  $z=d$  ( $\tilde{E}_T, \tilde{J}_T$ ) are the electric fields and the surface current densities in the film ( $\tilde{E}_T^i, \tilde{J}_T^i$ ) and out of the film ( $\tilde{E}_T^o, \tilde{J}_T^o$ ) respectively.

$$\tilde{E}_T = \tilde{E}_T^i + \tilde{E}_T^o \quad (16)$$

$$\tilde{J}_T = \tilde{J}_T^i + \tilde{J}_T^o \quad (17)$$

Using the complex resistive boundary condition, the characteristic matrix is determinate

$$\begin{bmatrix} \tilde{E}_x \\ \tilde{E}_y \end{bmatrix} = \begin{bmatrix} (G_{xx} - Z_s) & G_{xy} \\ G_{yx} & (G_{yy} - Z_s) \end{bmatrix} \cdot \begin{bmatrix} \tilde{J}_x \\ \tilde{J}_y \end{bmatrix} \quad (18)$$

The Galerkin moment method is implemented in the Fourier transform domain to reduce the integral equation to a matrix equation. The surface current **J** on the patch is expanded into a finite series of known basis functions  $J_{xm}$  and  $J_{ym}$

$$J = \sum_{n=1}^N a_n \begin{bmatrix} J_{xn} \\ 0 \end{bmatrix} + \sum_{m=1}^M b_m \begin{bmatrix} 0 \\ J_{ym} \end{bmatrix} \quad (19)$$

Where  $a_n$  and  $b_m$  are the mode expansion coefficients to be sought, substituting the vector Fourier transforms. Next, the resulting equation is tested by the same set of basic functions that was used in the expansion of the patch current. Thus, the integral equation is discredited into the following matrix equation

$$\begin{bmatrix} (\bar{Z}_{kn}^1)_{N \times N} & (\bar{Z}_{km}^2)_{N \times M} \\ (\bar{Z}_{lm}^3)_{M \times N} & (\bar{Z}_{ln}^4)_{M \times M} \end{bmatrix} \begin{bmatrix} (a_n)_{N \times 1} \\ (b_m)_{M \times 1} \end{bmatrix} = \begin{bmatrix} 0 \\ 0 \end{bmatrix} \quad (20)$$

$$Z_{kn}^1 = \int_{-\infty}^{+\infty} \int_{-\infty}^{+\infty} \tilde{J}_{xk}(-k_x, -k_y) \cdot (G_{xx} - Z_s) \tilde{J}_{xm}(k_x, k_y) dk_x dk_y$$

$$Z_{km}^2 = \int_{-\infty}^{+\infty} \int_{-\infty}^{+\infty} \tilde{J}_{xk}(-k_x, -k_y) \cdot G_{xy} \tilde{J}_{ym}(k_x, k_y) dk_x dk_y$$

$$Z_{lm}^3 = \int_{-\infty}^{+\infty} \int_{-\infty}^{+\infty} \tilde{J}_{yl}(-k_x, -k_y) \cdot G_{yx} \tilde{J}_{xm}(k_x, k_y) dk_x dk_y$$

$$Z_{ln}^4 = \int_{-\infty}^{+\infty} \int_{-\infty}^{+\infty} \tilde{J}_{yl}(-k_x, -k_y) \cdot (G_{yy} - Z_s) \tilde{J}_{yn}(k_x, k_y) dk_x dk_y$$

The existence of non trivial solution of (20) requires that

$$\det(\bar{Z}(f)) = 0 \quad (21)$$

Equation (21) is the characteristic equation for the complex resonant frequency of the generalized microstrip structure illustrated in Fig. 1. Where  $\bar{Z}$  is the matrix in (20).

### 3. Numerical Results and Discussion

The patch dimension is  $a=1630\mu\text{m}$ ,  $b=935\mu\text{m}$  and thickness  $R=350\text{nm}$ , using HTS materials YBCO with a critical temperature  $T_C$  of 89 K, a zero-temperature penetration depth of  $\lambda_0=140\text{ nm}$  and a normal state conductivity of  $\sigma_n=10^6\text{ s/m}$ . The substrate used in this study was lanthanum aluminate (LaAlO<sub>3</sub>), which has a good lattice match with YBCO [11]. LaAlO<sub>3</sub> have a relatively high dielectric constant for microwave and antenna applications, and the characteristics of the substrate often changes with temperature, this variation in the dielectric constant of LaAlO<sub>3</sub> causes uncertainty and variation in the resonant frequency of microstrip antennas. The permittivity of LaAlO<sub>3</sub> as a function of temperature is shown in Fig. 2, which it's given by Richard et al. [4].

Fig. 3 shows the calculated resonant frequency of an HTS antenna. The resonant frequency of HTS antennas rapidly increased below the critical temperature and showed 28.87 GHz at 80 K. After this temperature the increase of the resonant frequency was slow and stable at 28.95 GHz. Excellent agreements between our results and those measured by Richard et al. [4] are observed.

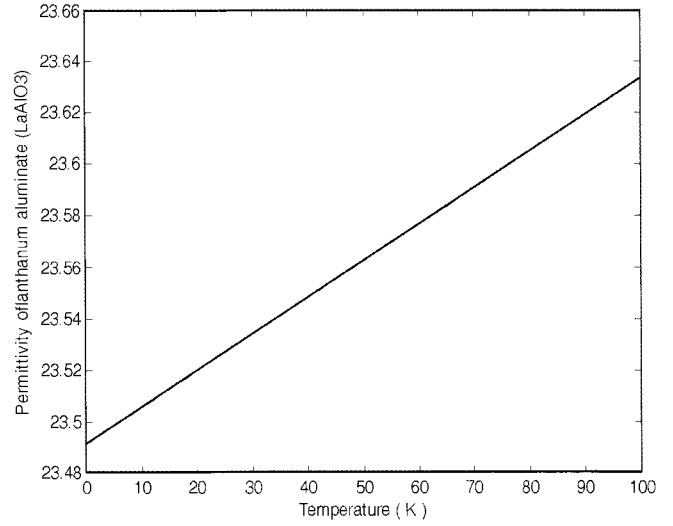


Fig. 2. Permittivity of lanthanum aluminate (LaAlO<sub>3</sub>)

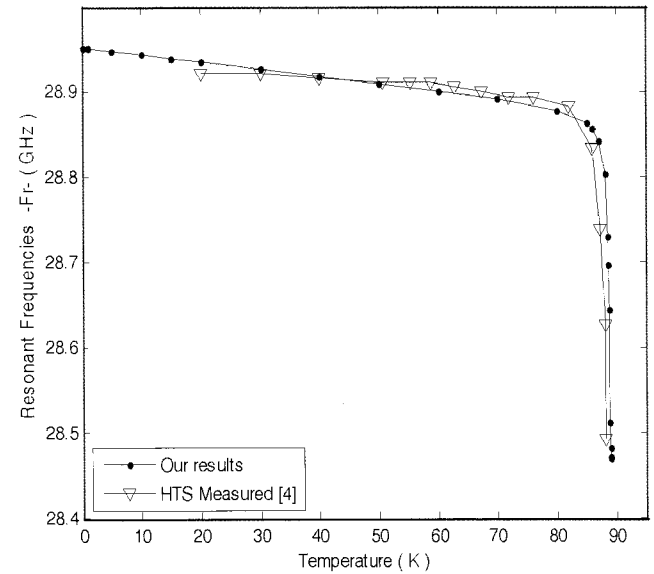
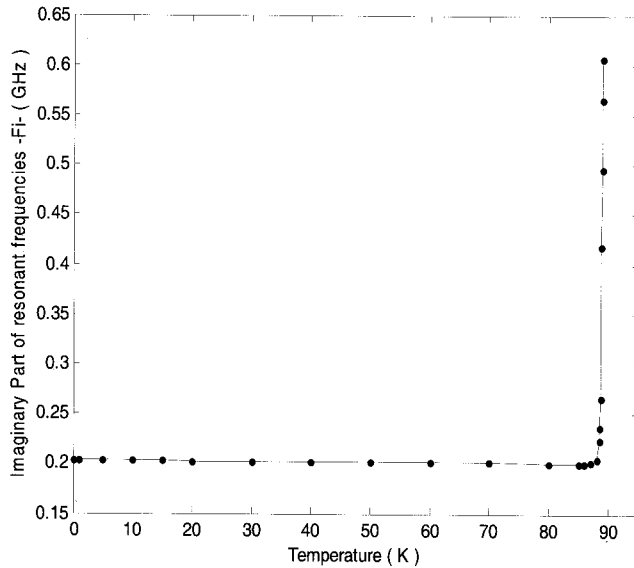


Fig. 3. Resonant frequency for a microstrip superconducting patch antenna as a function of the operating temperature, T

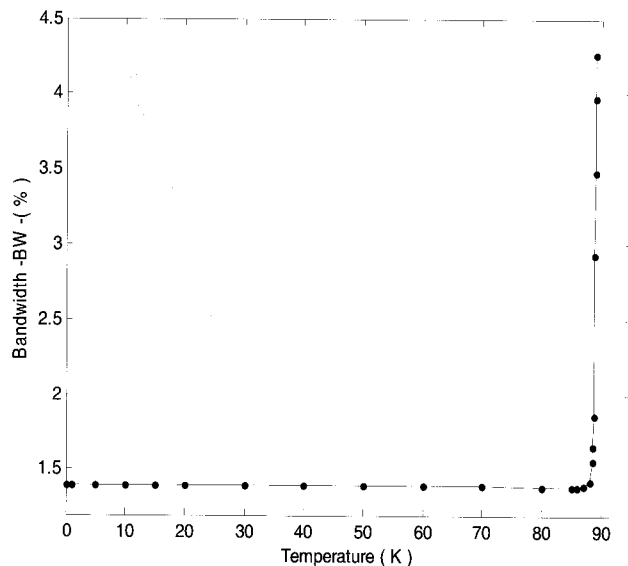
We show in Fig. 4 the imaginary part of resonant frequency versus the operating temperature T. It is seen that the imaginary part is 0.60 GHz at around 89 K. It decreases as the temperature is reduced under the  $T_C$ , and showed 0.20 GHz at around 87 K. After this point, the variation in the imaginary part could not be observed until 0 K.

Fig. 5 shows the bandwidth of an HTS antenna. The bandwidth curves for HTS antennas were similar in their dependence on temperature to the imaginary part of resonant frequency curves. The bandwidth of HTS antennas rapidly decreased below the critical temperature from 4.26% to 1.39% at 87 K. After this temperature, the decrease in bandwidth was slow and stable at 1.40%. The same behavior was observed experimentally by Richard et al. As a result, we can say that Silva result's are wrong.

From the above observations, it should be noted that the properties of the HTS antenna was stable at temperatures slightly lower than the critical temperature.



**Fig. 4.** Imaginary Part of resonant frequencies of rectangular microstrip superconducting patches as a function of the operating temperature,  $T$



**Fig. 5.** Bandwidth for HTS microstrip antenna as a function of the operating temperature,  $T$

#### 4. Conclusion

A rigorous full-wave analysis of a rectangular microstrip patch using superconducting materials has been presented. The problem has been formulated in terms of integral equations using vector Fourier transforms. An effi-

cient technique has been used for determining the dyadic Green's functions. Galerkin's method has been used to solve the surface current density on the rectangular patch. The calculated results have been compared with those previously measured and available in various literature, and excellent consistency has been found. From our work, we can confirm that the properties of the HTS antenna were stable at temperatures slightly lower than the critical temperature.

#### References

- [1] Sekiya, N., Kubota, A., Kondo, A., Hirano, S., Saito, A., and Ohshima, S., "Broadband superconducting microstrip patch antenna using additional gap-coupled resonators", *Physica C* 445-448 P. 994-997(2006).
- [2] Cassinese, A., Barra, M., Fraga, I., Kusunoki, M., Malandrino, G., Nakagawa, T., Perdicaro, L.M.S., Sato, K., Ohshima, S., and Vaglio, R., "Superconducting antennas for telecommunication applications based on dual mode cross slotted patches", *Physica C* 372-376 P.500-503 (2002).
- [3] Klopman, B.B.G., and Rogalla, H., "The propagation characteristics of wave-guiding structures with very thin superconductors; Application to coplanar wave-guide YBa<sub>2</sub> Cu<sub>3</sub>O<sub>7-x</sub> resonators", *IEEE Trans. Microwave Theory Tech.*;vol. MTT-41, no. 5, p. 781-791, 1993.
- [4] Richard, M.A., Bhasin, K.B., and Clapsy, P.C., "Superconducting microstrip antennas: An experimental comparison of two feeding methods", *IEEE Trans. Antennas Propagat.*, vol. AP-41, no. 7, pp. 967-974,1993.
- [5] da Silva, S. G., d'Assuao, A. G., and Oliveira, J. R.S., "Analysis of high T<sub>c</sub> superconducting microstrip antennas and arrays", *SBMO/IEEE MTT-S IMOC*. 1999.
- [6] Fortaki, T., Khedrouche, D., Bouttout, F., and Benghalia, A., "Vector Hankel transform analysis of a tunable circular microstrip patch", *Commun. Numer. Meth. Engng.* 2005; p 219-231.
- [7] Itoh, T., "A full-wave analysis method for open microstrip structures", *IEEE Trans. Antennas Propagat.*, v. AP-29, n. 1, pp. 63-67, 1981.
- [8] Cai, Z., and Bornemann, J., "Generalized spectral-domain analysis for multilayered complex media and high-T<sub>c</sub> superconductor applications", *IEEE Trans. Microwave Theory Tech.*, vol. MTT-40, no. 12, pp. 2251-2257, 1992.
- [9] Pozar, D. M., "Radiation and scattering from a microstrip patch on a uniaxial substrate", *IEEE Trans Antenna Propagat* AP-35, P.613-621 (1987).
- [10] Fortaki, T., and Benghalia, A., "Rigorous Full-wave analysis of rectangular microstrip patches over ground planes with rectangular apertures in multilayered substrates that contain isotropic and uniaxial aniso-

tropic materials", Microwave and Technology Letters vol. 41 no.6, June 2004.

- [11] Morrow, Jarrett D., Williams, Jeffery T., Davis, Mathew F., Licon, Darian L., Rampersad, H. R., Jazdyk, David R., Zhang, Xiaoping, Long, Stuart A., and Wolfe, John C., "Circularly Polarized 20-GHz High-Temperature Superconducting Microstrip Antenna Array", IEEE Transactions on Applied Superconductivity, vol. 9, no. 4, December 1999.



sion and Distribution.

**Fouad Chebbara Hong** received his engineering degree in Electronics Option Communication from the University of Batna (Alegria) and his Magistere in Electronics Option Microwave from the University of Constantine (Algeria) His research interests are antennas, microbande and Transmis-